95−670 GHz EPR Studies of Canthaxanthin Radical Cation Stabilized on a Silica−Alumina Surface

Tatyana A. Konovalova,[†] J. Krzystek,[‡] Peter J. Bratt,[§] J. van Tol,[‡] Louis-Claude Brunel,[‡] and Lowell D. Kispert*[,†]

Department of Chemistry, P.O. Box 870336, University of Alabama, Tuscaloosa, Alabama 35487, Center for Interdisciplinary Magnetic Resonance, National High Magnetic Field Laboratory, Florida State University, Tallahassee, FL 32310, Department of Chemistry, P.O. Box 117200, University of Florida, Gainesville, FL 32611, and The Department of Biology, Darwin Building, University College London, Gower Street, London WC1H 9EW, United Kingdom

Received: February 16, 1999; In Final Form: April 27, 1999

The 95−670 GHz EPR measurements at 5 K were performed on canthaxanthin radical cation chemically generated on silica−alumina. The 327 GHz and higher frequency EPR spectra were resolved into two principal components of the *g* tensor. Spectral simulation indicated this to be the result of *g* anisotropy where $g_{\|} = 2.0032$ and $g_{\perp} = 2.0023$. This type of *g* tensor is consistent with the theory for polyacene π-radical cations, which states that the *g* tensor becomes cylindrically symmetric with increasing chain length. This also demonstrates that the symmetrical unresolved EPR line at 9 GHz is due to a carotenoid π-radical cation with electron density distributed throughout the whole chain as predicted by RHF−INDO/SP molecular orbital calculations. The lack of temperature dependence of the EPR line widths over the range of 5−80 K at 327 GHz suggests rapid rotation of methyl groups even at 5 K that averages out the proton couplings from three oriented β-protons. In fact, similar line widths at 5 K were observed at 670 GHz. Simulation of EPR spectra at 95−250 GHz gives only symmetrical unresolved lines. The present work shows that the 327−670 GHz EPR measurements are sufficient to resolve the individual *g* tensors of C−H containing π-radicals in powder and frozen glasses. Symmetry differences can be deduced from which radical identification can be made.

Introduction

Canthaxanthin, 4,4′-dioxy-β-carotene, belongs to the carotenoid family of molecules. Carotenoids are present in photosynthetic reaction centers and light-harvesting membranes.[1,2] They play an important photoprotective role by intercepting chlorophyll triplet species and preventing the formation of damaging singlet oxygen.[3,4] The light-absorbing properties of the carotenoids derive from the presence of a long chain of conjugated double bonds. The large number of double bonds leads to the absorption of light in the visible region, and this energy can be transferred to the bacteriochlorophyll a (Bchl a)-based antenna systems.[5−7] X-ray data indicate that in light-harvesting protein complexes, carotenoids appear to be in van der Waals contact with two Bchl a rings.[8,9] This close association and extended π-electron system of carotenoids determine their active participation in the electron transfer processes in photosynthetic reaction centers (RC). Carotenoid radical cations ($Car^{\bullet+}$) have been detected optically in the PSII reaction center.[10,11] To understand the mechanism of the $Car^{\bullet+}$ formation in the RC, detailed information regarding the electronic structure of carotenoids and their oxidation products is required. Carotenoid radical cations, generated electrochemically, are relatively short-lived in solution.[12] However, when prepared on silica−alumina surfaces they are stable for hours at room temperature.[13,14] The electron transfer reaction of carotenoids adsorbed on a surface, where molecular motion is restricted, is expected to be a good model for reactions in the photosynthetic reaction center where carotenoids are surrounded by proteins.

It has been shown that electron paramagnetic resonance (EPR) spectroscopy is a sensitive and informative technique for investigation of photosynthetic electron transport.[15,16] This method is now being extended by using electron nuclear double resonance (ENDOR)[17,18] and electron spin−echo envelope modulation (ESEEM)[19,20] spectroscopy. The X-band (9 GHz) EPR spectrum of a carotenoid radical cation consists of an unresolved single line with $g_{iso} = 2.0027 \pm 0.0002$ and line width $\Delta H_{pp} = 13.6 \pm 0.5$ G in solution (simultaneous electrochemical EPR study)[21] and 15.0 ± 1.0 G for $Car^{\bullet+}$ adsorbed on solid supports.[13] The *g* value (2.0027) is characteristic for organic π-radicals.[22] The line shape most closely resembles that of a Gaussian line, which indicates that the line is inhomogeneously broadened by unresolved proton hyperfine structure. ENDOR spectroscopy was used to measure the hyperfine interactions in canthaxanthin radical cation adsorbed on silica−alumina (Scheme 1).[13] That study revealed the hyperfine coupling constants of the β-protons of methyl groups attached to the carbon atoms C(5, 5′), C(9, 9′) and C(13, 13′).[13] It was shown that the methyl groups of adsorbed canthaxanthin are freely rotating at 120 K, and even any small anisotropy is averaged out.

High-field EPR spectroscopy greatly improves the resolution of the EPR signals for spectral features such as the *g* tensor. Deviations of the *g* value from free electron $g = 2.0023$ are due to spin−orbital interactions, which are one of the most important structural characteristics.[23] Using a higher frequency

* To whom correspondence should be addressed.
[†] University of Alabama.
[‡] Florida State University.
[§] University College London.

10.1021/jp990579r CCC: $18.00
Published on Web 06/24/1999

SCHEME 1. Total Spin Density Distribution in the Canthaxanthin Radical Cation

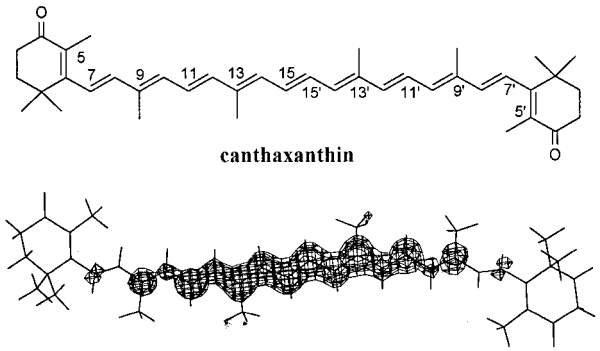

results in enhanced spectral resolution in accordance with the resonance equation

$$H = h\omega/2\pi g\beta \quad (1)$$

where h is the Planck constant, β is the Bohr magneton, and ω is the frequency of electromagnetic radiation. If paramagnetic centers with different g values are present, the difference in the field positions of the resonances is proportional to ω

$$\delta H = h\omega/2\pi\beta \times (1/g_1 - 1/g_2) \quad (2)$$

Recently a number of HF-EPR investigations on the photosynthetic RC primary electron donors were carried out. These experiments increased what was known about the electron structure of these molecules. The W-band (95 GHz) studies of the primary donor radical cation $P_{865}^{\bullet+}$ in single crystals of *Rhodobacter sphaeroides* R-26[24] indicated the presence of two magnetically inequivalent sites in the unit cell of the crystals. The W-band EPR measurements on single crystals of deuterated $P_{865}^{\bullet+}$ showed essential resolution of the EPR spectrum into its three principal components.[25] Use of 325 GHz gave well-resolved EPR spectra of the radical cation of the chlorophyll dimer $P_{700}^{\bullet+}$ observed without prior deuteration.[26] HF-EPR data demonstrated that $P_{700}^{\bullet+}$ showes less g anisotropy with increasing temperature.[26]

X-band EPR and ENDOR results on the canthaxanthin radical cation suggest that $Car^{\bullet+}$ is a π-radical cation in which the electron density is distributed over the whole polyene chain as predicted by RHF−INDO/SP MO calculations.[27,28] In this paper we report 95-670 GHz EPR measurements of canthaxanthin radical cations adsorbed on silica−alumina. The main reason for using HF-EPR spectroscopy was to determine the principal components of the g tensor of $Car^{\bullet+}$, which is a function of electron delocalization, and thus distinguish it from the powder spectra of other C−H containing π-radicals.

Experimental Section

Canthaxanthin, supplied by Fluka, was stored at −14 °C in a desiccator containing drierite. The purity of the samples was determined by ^{1}H NMR (360 MHz, $CDCl_3$) and TLC analysis.

The solvent, methylene chloride (CH_2Cl_2) (Aldrich, anhydrous), was stored under nitrogen in a drybox and used without further purification.

Silica−alumina (Aldrich, Al_2O_3 = 13%) was activated by heating at 570 °C for 3−12 h in air in an open ceramic "boat", then cooling to 50 °C and storing in a desiccator. Carotenoid solutions in CH_2Cl_2 (10^{-2} to 10^{-3} M) were degassed in quartz EPR tubes by three freeze−pump−thaw cycles. An appropriate amount of fresh activated silica−alumina was then added to the carotenoid solution contained in an EPR tube. Quartz EPR tubes of o.d. 4 mm and 8 mm were used for the 9.5 GHz and higher frequency measurements, respectively. The solvent was evaporated under reduced pressure, and the tube was evacuated and sealed. The samples were stored at 77 K.

The X-band (9 GHz) EPR spectra were measured on a Bruker ESP300 spectrometer. The HF-EPR measurements were carried out at the high-field EMR facility of the National High Magnetic Field Laboratory (Tallahassee, Florida). The 95−440 GHz measurements were performed on a spectrometer analogous to that described by Mueller et al.[29] It has been briefly described,[30] and will be elaborated on in a forthcoming paper.[31] The spectrometer has fundamental microwave frequencies of 95 ± 3 and 110 ± 3 GHz produced by two Gunn oscillators, from which higher harmonics can be also generated to yield the multiplicities of these frequencies. A set of high-pass filters removes the fundamentals and lower harmonics. The fundamental frequency was measured using an EIP 578B counter. The magnet used was an Oxford Instruments Teslatron consisting of a main set of superconducting coils that can be put in persistent mode in the vicinity of resonance and a smaller superconducting sweep coil operating in nonpersistent mode and allowing a field sweep of ± 0.1 T with respect to the persistent field. The 670 GHz experiments were carried out in another home-built spectrometer, which used a far-infrared laser (Edinburg Instruments FIR-100) as source. The active medium was deuterated methyl iodide (Aldrich). This spectrometer used a resistive Bitter-type magnet of improved stability and homogeneity (the latter equal to 10^{-5} in a 1 cm sphere) which could reach a maximum field of 25 T (the so-called "Keck" magnet). Both spectrometers operated in a single-pass transmission mode (no resonator employed).

In both types of experiments, the sample in a sealed quartz tube fitting the oversized stainless steel waveguide (i.d. 9.6 mm) was placed within an Oxford Instruments CF 1200 continuous flow cryostat. Approximate sample volume was 500 mm^3. A liquid helium cooled hot-electron InSb bolometer (QMC Instruments, U.K.) was used as a power detector to measure the mm- and submm-wave absorption through the sample. The spectra were recorded in the first derivative mode, using 8 kHz magnetic field modulation. The typical magnetic field sweep rate was 60 G/min. To calibrate and confirm the linearity of the magnetic field over the sweep width, a polycrystalline standard sample of MnO in MgO was used as a field marker according to the method described by Burghaus et al.[32]

Results and Discussion

The high-field EPR spectra (Figure 1, solid lines) of canthaxanthin adsorbed on silica−alumina were measured at 94.6, 327.0, 373.6, 439.2, and 670.5 GHz at 5 K. Compared to the X-band (9 GHz) signal, the spectra at and above 327.0 GHz become resolved into two components. The 670 GHz spectrum exhibits maximum line separation.

The g tensor of the canthaxanthin radical cation was determined by simulating the experimental spectra. The corrected field positions of the spectra were defined by calibrating the field with the Mn^{2+} standard. The spectra were simulated with reasonable accuracy by using experimental line widths at 9 GHz, the known Larmor frequency, the corrected field positions, and the proton hyperfine coupling constants for the canthaxanthin radical cation obtained previously (Table 1).[13] Assignment of the coupling constants to specific methyl protons was based on a comparison of the experimental and simulated spectra. Parameters for the simulation were obtained from the

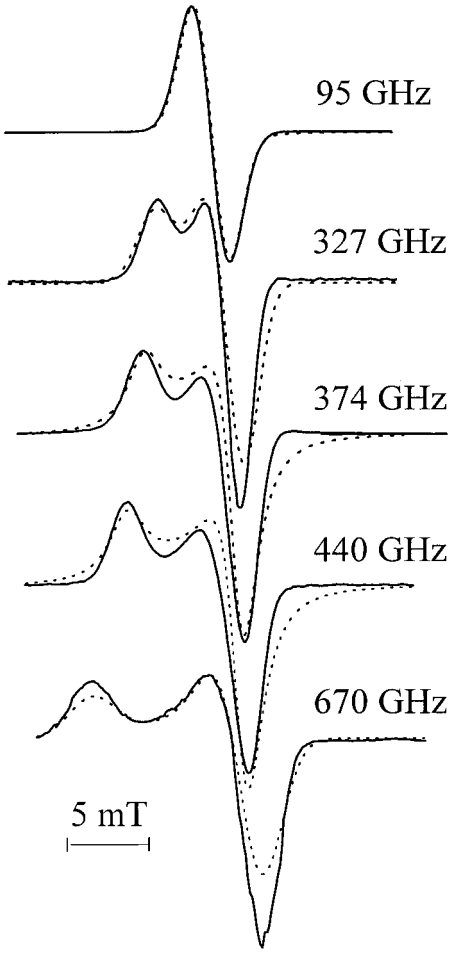

Figure 1. HF-EPR spectra of canthaxanthin radical cation adsorbed on silica−alumina: solid lines, experimental spectra recorded at 5 K; dotted lines, simulated spectra using g tensor values $g_{zz} = 2.0032$ and $g_{xx} = g_{yy} = 2.0023$ and line width of 13.6 G.

TABLE 1: Experimental and RHF-INDO/SP Calculated β-Proton Couplings (MHz): Comparison of Canthaxanthin Radical Cation and CH_3•CHCOOH Radical

	ENDOR couplings in solution[a]		ENDOR couplings in solid[b]			
β-protons	simulated A_{iso}	calcd A_{iso}	A_{xx}	A_{yy}	A_{zz}	calcd A_{iso}
canthaxanthin $RC^{\bullet+}$						
C_5-$C_\beta H_3$	2.2	2.1; 2.2	1.9	1.9	2.0	2.1; 2.2
C_9-$C_\beta H_3$	8.3	8.1; 8.5	8.2	8.2	8.5	8.1; 8.5
C_{13}-$C_\beta H_3$	13.0	13.1; 13.4	13.0	13.0	13.0	13.1; 13.4
CH_3•CHCOOH in alanine crystal[c]	**300 K**		**77 K**			
$H_{\beta 1}$	70		116	118	128	120
$H_{\beta 2}$	70		77	76	77	76
$H_{\beta 3}$	70		11	16	14	14

[a] Ref 28. [b] Ref 13. [c] Ref 38.

RHF−INDO/SP semiempirical MO calculations[33,34] carried out on AM1 geometry optimized structures.[27,28] The principal components of the g tensor for Car•+ are found to be $g_{zz} = 2.0032 \pm 0.0001$ and $g_{xx} = g_{yy} = 2.0023 \pm 0.0001$. The simulated spectra are shown in Figure 1, dotted lines. The agreement between simulated and experimental spectra is generally good, although small deviations are visible. Of the possible reasons for these deviations we have found that admixture of dispersion to the spectra is primarily responsible (the high field spectrometers employed do not allow to discriminate completely absorption and dispersion). We have not observed either saturation or fast passage effects which in principle could contribute to line shape deformations.

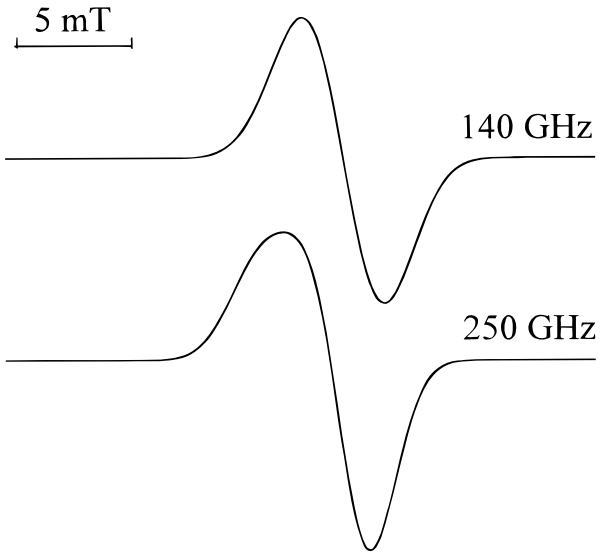

Figure 2. Simulated HF-EPR spectra of adsorbed canthaxanthin radical cation at 140 and 250 GHz using g tensor values $g_{zz} = 2.0032$ and $g_{xx} = g_{yy} = 2.0023$ and line width of 13.6 G.

TABLE 2: Comparison of g Values for Various Radical Cations with Those Observed for Canthaxanthin Radical Cation

radical cations	g_{xx}	g_{yy}	g_{zz}	g_{iso}	structure	ref
$TP^{\bullet+}/AsF_6^-$	2.0031	2.0028	2.0022	2.0027	polymer	35
$TP^{\bullet+}/PF_6^-$	2.00312	2.00230	2.00206	2.00249	stacked array	36
$QP^{\bullet+}/PF_6^-$	2.00217	2.00217	2.00310	2.00248	stacked array	36
$P_{865}^{\bullet+}$	2.00337	2.00248	2.00208	2.00264	dimer	25
$P_{700}^{\bullet+}$	2.00317	2.00260	2.00226	2.0027	dimer	26
Bchl $a^{\bullet+}$	2.0033	2.0026	2.0022	2.0027	monomer	24
$Car^{\bullet+}$	2.0023	2.0023	2.0032	2.0026	symmetr. π-$RC^{\bullet+}$	present work

Simulated 140 and 250 GHz EPR spectra which were not obtained experimentally are shown in Figure 2. Spectral simulations using $g_{||} = 2.0032$, $g_\perp = 2.0023$, and line width of 13.6 G showed that the canthaxanthin radical cation cannot be resolved at these frequencies. At 140 GHz the $Car^{\bullet+}$ signal is symmetrical and exists as an unresolved line. At 250 GHz it becomes slightly asymmetrical. Determination of g tensor components from resolved 327−670 GHz EPR spectra allows differentiation between carotenoid radical cations and other C−H π-radicals which possess different symmetry. It is interesting to compare the above g values for the canthaxanthin radical cation with the principal g-tensor components reported for other organic radical cations (see Table 2). Warming of *p*-terphenyl (TP) doped with excess AsF_5 causes polymerization to give highly conducting charge-transfer salts ($AsF_6^-/TP^{\bullet+}$).[35] The observed EPR signal has $g_{iso} = 2.0027$ with principal components of the g tensor $g_{xx} = 2.0031$, $g_{yy} = 2.0028$, $g_{zz} = 2.0022$. The EPR spectra of single crystals of the conducting PF_6^- salts of TP and *p*-quaterphenyl (QP) radical cations have the isotropic g value 2.0025.[36] The difference in the g_{iso} values for $AsF_6^-/TP^{\bullet+}$ and $PF_6^-/TP^{\bullet+}(QP^{\bullet+})$ is due to a different mechanism of electron exchange in these salts. While in the $AsF_6^-/TP^{\bullet+}$ salt, electron exchange occurs along its polymer structure, the PF_6^- salts of TP and QP radical cations exist in columnar stacks of aromatic rings, and rapid electron exchange occurs across the stack. The difference $g_{xx} - g_{yy}$ is smaller for the AsF_6^-salt of TP radical cation than for the $PF_6^-/TP^{\bullet+}$ (g_{xx}

$= 2.00312$, $g_{yy} = 2.00230$, $g_{zz} = 2.00206$). It should be noticed that the chain length is considerably longer in the $AsF_6^-/TP^{\bullet+}$ than in the $PF_6^-/TP^{\bullet+}$ salt. The PF_6^- salt of QP radical cation exhibits the g tensor with $g_{xx} = 2.00217$, $g_{yy} = 2.00217$, $g_{zz} = 2.00312$. The appearance of cylindrical symmetry for the g tensor of the QP radical cation salt is consistent with the Stone theory[37] for polyacenes, which states that the difference $g_{xx} - g_{yy}$ decreases with increasing chain length. When $g_{xx} - g_{yy}$ approaches zero, the g tensor becomes cylindrically symmetrical with $g_{xx} = g_{yy} = g_\perp$ and $g_{zz} = g_{||}$.

The cylindrical symmetry for the all-trans carotenoids is not surprising because these molecules are long straight chain polyenes. The principal components of the g tensor for $Car^{\bullet+}$ differ from those of other radical cations found in photosynthetic RC, which are practically identical within experimental error (Table 2)[24−26] and exhibit large differences between g_{xx} and g_{yy} values. The similarity of g values of $P_{865}^{\bullet+}$ in single crystals of *R. sphaeroides* R-26 (2.00337, 2.00248, and 2.00208),[25] the chlorophyll dimer $P_{700}^{\bullet+}$ (2.00317, 2.00260, and 2.00226),[26] and the monomeric Bchl a radical cation (2.0033, 2.0026, and 2.0022)[24] would indicate similar electron density distribution in these molecules. For all of these systems asymmetric electronic structures have been suggested. A different behavior is expected for the carotenoid radical cation. Scheme 1 shows the total spin-density distribution for the canthaxanthin radical cation calculated by the UHF−INDO semiempirical method based on AM1 geometry optimized structure.

Temperature dependence of the line width for the $Car^{\bullet+}$ signal was measured at 327 GHz. It was found that the spectra of canthaxanthin radical cation show no measurable difference in line widths between 80 and 5 K. Previous ENDOR studies[13,27] indicated that the line width of $Car^{\bullet+}$ is determined primarily by methyl proton hyperfine splittings. The coupling constants of a rotating and nonrotating methyl group are different. In the known example of the CH_3•CHCOOH radical generated by γ-irradiation of single crystal of *l*-α-alanine[38] at 300 K, the three β-protons of a freely rotating CH_3 group are equivalent and have an isotropic hyperfine coupling constant (70 MHz). However, upon cooling this system to 77 K, different isotropic coupling constants were obtained for each β-proton (120, 76, and 14 MHz with an average value 70 MHz).[38] Different interaction of the unpaired electron with the three methyl protons has been interpreted in terms of restriction of free rotation of the methyl groups at low temperatures. The absence of measurable change in the line width (and, hence, in the coupling constants) of $Car^{\bullet+}$ from 80 to 5 K indicates that the methyl groups of adsorbed carotenoid radical cation are freely rotating even at 5 K. In some cases the methyl groups can undergo tunneling rotation. When the activation barrier (V_{barr}) is low enough and the tunneling frequency (ν_t) is high enough, such a process occurs. For instance, it has been found that the CH_3 group in an irradiated single crystal of methylmalonic acid undergoes nearly free rotation at 4.2 K.[39] EPR, ENDOR, and ELDOR studies of irradiated crystals of 2,2,5-trimethyl-1,3-dioxane-4,6-dione have shown that the methyl group undergoes tunneling rotation below 30 K where $\nu_t = 830$ MHz and $V_{barr} = 0.8$ kcal/mol.[40] Thus, at 4−30 K the four-line EPR spectrum observed at higher temperatures and corresponding to three equivalent methyl protons changes to a seven-line spectrum.[40] Such a spectral change was attributed to a rapidly tunneling methyl group because the ground vibrational state is split into three levels due to the 3-fold rotational barrier of the CH_3-group. Types of intermolecular motion other than tunneling have not been extensively investigated. Since we did not observe any spectral changes with temperature from 80 to 5 K, we can suggest that carotenoid radical cation methyl groups, rapidly rotating at low temperatures, appear not to undergo tunneling rotation.

Conclusions

In the present study we report the first example of well-resolved high-field (327−670 GHz) EPR spectra of a carotenoid radical cation. The X-band (9 GHz) EPR spectrum of the canthaxanthin radical cation adsorbed on silica−alumina exhibits only an unresolved symmetrical single line with a g value of 2.0027. The two principal components of the g tensor were found by spectral simulation at 327−670 GHz to be $g_{||} = 2.0032$ and $g_\perp = 2.0023$. Cylindrical symmetry for the g tensor is consistent with the Stone theory for polyacenes. Comparison of the principal g tensor components obtained by spectral simulation for canthaxanthin radical cation ($g_{||}$ and $g_\perp$) with those observed for arene radical cations TP and QP and other radical cations demonstrates that the carotenoid radical cations do not form a stacked array in which electron exchange could occur. This also demonstrates that $Car^{\bullet+}$ is a π-radical cation with unpaired electron density distributed throughout the polyene chain. The lack of temperature dependence of the EPR line widths over the range of 5−80 K indicates rapid rotation of methyl groups even at 5 K so that the proton couplings from the three β-protons are averaged. No evidence of tunneling rotation was obtained. Spectral simulations at 95−250 GHz give only unresolved single lines. At 9−250 GHz the carotenoid radical cation cannot be distinguished from other C−H π-radicals observed in powders and frozen glasses, since its g tensor cannot be resolved at these frequencies. The present work shows that the 327−670 GHz EPR measurements are sufficient to resolve the individual g tensor components and distinguish carotenoid radical cations from other C−H containing radicals, which have different symmetry.

Acknowledgment. This work was supported by the Division of Chemical Sciences, Office of Basic Energy Sciences, Office of Energy Research, the U.S. Department of Energy, Grant DE-FG02-86ER13465 and the National High Magnetic Field Laboratory. We thank Dr. Alexander Shubin for providing the ESR-1 simulation program. Special thanks go to Dr. Elli Hand for helpful discussion.

References and Notes

(1) Lawlor, D. W. In *Photosynthesis: Metabolism, Control and Physiology*; Wiley: New York, 1987.

(2) Goodwin, T. W. In *The Biochemistry of the Carotenoids: Plants*; Chapman and Hall: London, 1980.

(3) Koyama, Y. *J. Photochem. Photobiol. B* **1991**, *9*, 265.

(4) Bensassson, R. V.; Land, E. J.; Truscott, T. G. *Excited States and Free Radicals in Biology and Medicine*; Oxford University Press: Oxford, 1993.

(5) Frank, H. A.; Cogdell, R. J. In *Carotenoids in Photosynthesis*; Young, A., Britton, G., Eds.; Chapman and Hall: London, 1993.

(6) Mimuro, M.; Katoh, T. *Pure Appl. Chem.* **1991**, *63*, 123.

(7) Britton, G.; Liaaen-Jensen, S.; Pfander, H. In *Carotenoids B: Spectroscopy*; Birkhäuser Verlag: Basel, 1995.

(8) McDermott, G.; Prince, S. M.; Freer, A. A.; Hawthornethwaite-Lawless, A. M.; Papiz, M. Z.; Cogdell, R. J.; Isaacs, N. W. *Nature* **1995**, *374*, 517.

(9) Freer, A. A.; Prince, S. M.; Sauer, K.; Papiz, M. Z.; Hawthornethwaite-Lawless, A. M.; McDermott, G.; Cogdell, R. J.; Isaacs, N. W. *Structure* **1996**, *4*, 449.

(10) Mathis, P.; Rutherford, A. W. *Biochim. Biophys. Acta* **1984**, *767*, 217.

(11) Telfer, A.; De Las Rivas, J.; Barber, J. *Biochim. Biophys. Acta* **1991**, *1060*, 106.

(12) Grant, J. L.; Krammer, V. J.; Ding, R.; Kispert, L. D. *J. Am. Chem. Soc.* **1988**, *110*, 2151.

(13) Jeevarajan, A. S.; Kispert, L. D.; Piekara-Sady, L. *Chem. Phys. Lett.* **1993**, *209*, 269.

(14) Konovalova, T. A.; Kispert, L. D. *J. Chem. Soc., Faraday Trans.* **1998**, *94*, 1465.

(15) Miller, A.-F.; Brudvig, G. W. *Biochim. Biophys. Acta* **1991**, *1056*, 1.

(16) Dexheimer, S. L.; Klein, M. P. *J. Am. Chem. Soc.* **1992**, *114*, 2821.

(17) Plato, M.; Lubitz, W.; Lendzian, F. *Israel J. Chem.* **1988**, *28*, 109.

(18) Lubitz, W.; Isaacson, R. A.; Okamura, M. Y.; Abresch, E. C.; Plato, M.; Feher, G. *Biochim. Biophys. Acta* **1989**, *977*, 227.

(19) Käss, H.; Bittersmann-Weidlich, E.; Andreasson, L.-E.; Bönigk, B.; Lubitz, W. *Chem. Phys.* **1995**, *194*, 419.

(20) Davis, I. H.; Heathcote, P.; MacLachlan, D. J.; Evans, M. C. W. *Biochim. Biophys. Acta* **1993**, *1143*, 183.

(21) Khaled, M. M.; Hadjipetrou, A.; Kispert, L. D.; Allendoefer, R. D. *J. Phys. Chem.* **1991**, *95*, 2438.

(22) Wertz, J. E.; Bolton, J. R. *Electron Spin Resonance: Elementary Theory and Practical Applications*; McGraw-Hill: New York, 1972.

(23) Kevan, L.; Bowman, M. K. *Modern Pulsed and Continuous-Wave Electron Spin Resonance*; Wiley: New York, 1990.

(24) Burghaus, O.; Plato, M.; Bumann, D.; Neumann, B.; Lubitz, W.; Möbius, K. *Chem. Phys. Lett.* **1991**, *185*, 381.

(25) Klette, R.; Törring, J. T.; Plato, M.; Möbius, K.; Bönigk, B.; Lubitz, W. *J. Phys. Chem.* **1993**, *97*, 2015.

(26) Bratt, P. J.; Rohrer, M.; Krzystek, J.; Evans, M. C. W.; Brunel, L.-C.; Angerhofer, A. *J. Phys. Chem. B* **1997**, *101*, 9686.

(27) Piekara-Sady, L.; Khaled, M. M.; Bradford, E.; Kispert, L. D.; Plato, M. *Chem. Phys. Lett.* **1991**, *186*, 143.

(28) Piekara-Sady, L.; Jeevarajan, A. S.; Kispert, L. D. *Chem. Phys. Lett.* **1993**, *207*, 173.

(29) Mueller, F.; Hopkins, M. A.; Coron, N.; Grynberg, M.; Brunel, L. C.; Martinez, G. *Rev. Sci. Instrum.* **1989**, *60*, 3681.

(30) Krzystek, J.; Sienkiewicz, A.; Pardi, L.; Brunel, L.-C. *J. Magn. Reson.* **1997**, *125*, 207.

(31) Hassan, A.; Pardi, L.; Krzystek, J.; Sienkiewicz, A.; Rohrer, M.; Brunel, L. C., manuscript in preparation.

(32) Burghaus, O.; Rohrer, M.; Götzinger, T.; Plato, M.; Möbius, K. *Meas. Sci. Technol.* **1992**, *3*, 765.

(33) Plato, M.; Tränkle, E.; Lubitz, W.; Lendzian, F.; Möbius, K. *Chem. Phys.* **1986**, *107*, 185.

(34) Lendzian, F.; Lubitz, W.; Scheer, H.; Hoff, A. J.; Plato, M.; Tränkle, E.; Möbius, K. *Chem. Phys. Lett.* **1988**, *148*, 377.

(35) Robinson, T.; Kispert, L. D.; Joseph, J. *J. Chem. Phys.* **1985**, *82*, 1539.

(36) Kispert, L. D.; Joseph, J.; McGraw, J.; Robinson, T.; Drobner, R. *Synth. Met.* **1987**, *19*, 67.

(37) Stone, A. J. *Mol. Phys.* **1964**, *7*, 309.

(38) Horsfield, A.; Morton, J. R.; Whiffen, D. H. *Mol. Phys.* **1961**, *4*, 327, 425.

(39) Clough, S.; Hill, J.; Poldy, F. *J. Phys. C: Solid State Phys.* **1972**, *5*, 518.

(40) Geoffroy, M.; Kispert, L. D.; Hwang, J. S. *J. Chem. Phys.* **1979**, *70*, 4238.